

Climate constraint reflects forced signal

ARISING FROM P. M. Cox, C. Huntingford & M. S. Williamson *Nature* 553, 319–322 (2018); <https://doi.org/10.1038/nature25450>

A recent paper by Cox et al.¹ introduces $\bar{\Psi}$, “a theoretically informed metric of global temperature variability”, which scales with equilibrium climate sensitivity (ECS) across 16 general circulation models (GCMs). Cox et al.¹ report that $\bar{\Psi}$ provides a strong constraint on ECS, ruling out both high and low values. Our analysis shows that this constraint is sensitive to the GCMs considered, primarily reflects the forced climate response rather than climate variability and does not narrow the uncertainty in ECS. It is therefore premature to rule out the possibility of large ECS values. There is a Reply to this Comment by Cox, P. M. et al. *Nature* 563, <https://doi.org/10.1038/s41586-018-0641-x> (2018).

Cox et al.¹ build on fundamental physical principles, making use of the fluctuation–dissipation theorem, which relates the statistical properties of a system in thermal equilibrium to the sensitivity of the system to forcing. The authors apply the fluctuation–dissipation theorem to the ‘Hasselmann model’ of global climate under white-noise forcing. Using this highly idealized model, they define $\bar{\Psi}$ as the ratio of temperature variability to a measure of the one-year-lag autocorrelation of annual-mean temperature and show $\bar{\Psi}$ to be proportional to ECS. Their work extends previous research on the fluctuation–dissipation theorem and climate^{2–5} by demonstrating that $\bar{\Psi}$ scales with ECS in historical simulations performed with GCMs. Using the instrumental surface-temperature record as an observational constraint on $\bar{\Psi}$, Cox et al.¹ propose bounds on ECS that are narrower than in previous assessments. They provide what appear to be the essential ingredients⁶ for an emergent constraint on climate sensitivity: their metric $\bar{\Psi}$ is observable, scales with ECS values in GCMs and has a sound theoretical basis.

An implicit assumption by Cox et al.¹ is that $\bar{\Psi}$ primarily reflects internal climate variability. In simulations and observations of historical climate change, $\bar{\Psi}$ is also influenced by natural (volcanic and solar) and anthropogenic forcings. To determine whether $\bar{\Psi}$ scales with ECS in simulations without changes in external forcing, we use pre-industrial control experiments, in which global temperature variations are due to internal climate variability alone. Following Cox et al.¹, we calculate $\bar{\Psi}$ using de-trended, overlapping 55-year windows of global-mean surface

temperature. The average of the individual windows in an entire control simulation of a model is denoted by $\bar{\Psi}$. Consistent with the findings of Cox et al.¹ for historical simulations, a strong relationship exists between $\bar{\Psi}$ and ECS in GCM control experiments (Fig. 1a).

However, there is substantial spread in the regression between $\bar{\Psi}$ and ECS in individual segments of the control simulations. For consistency with the length of the historical record (1880–2016), we randomly sample 137-year periods from each pre-industrial control simulation, compute $\bar{\Psi}$ and then calculate the correlation between $\bar{\Psi}$ and ECS. Repeating this calculation, we find that only about 7% of our samples yield a relationship that rivals or exceeds the correlation coefficient found by Cox et al.¹ ($r = 0.77$). This result suggests that the observational record is too short to act as a strong ECS constraint⁷ and that forced temperature changes probably enhance the strength of the $\bar{\Psi}$ –ECS relationship in historical simulations.

Compared to the historical simulations used by Cox et al.¹ (Fig. 1b), the pre-industrial control simulations exhibit a different $\bar{\Psi}$ –ECS scaling (Fig. 1a), with a narrower range of $\bar{\Psi}$ values across GCMs. This difference in scaling has important implications. Applying the observational $\bar{\Psi}$ estimate to the pre-industrial control simulations yields a 95% confidence interval for the ECS of 2.6–5.4°C (Fig. 1a). This is substantially higher than that found by Cox et al.¹ using historical simulations (1.6–4.0°C; Fig. 1b). We therefore infer that the strong constraint on the high end of ECS reported by Cox et al.¹ arises primarily from the response to historical forcing, not from internal variability.

The physical derivation of the relationship between $\bar{\Psi}$ and ECS by Cox et al.¹ is valid only for stationary white-noise forcing. It is therefore important to remove forced temperature signals. Cox et al.¹ assume that forced temperature variability can be removed by linearly de-trending the temperature time series. An alternative method (which does not require this assumption) is to remove the ensemble-mean response of a model to external forcing. We contrast these two methods for signal removal using ten realizations of historical climate change from the CSIRO-Mk3-6-0 model (Fig. 2a). The approach of Cox et al.¹ yields $\bar{\Psi}$ values that are inflated after about 1950 relative to those based on

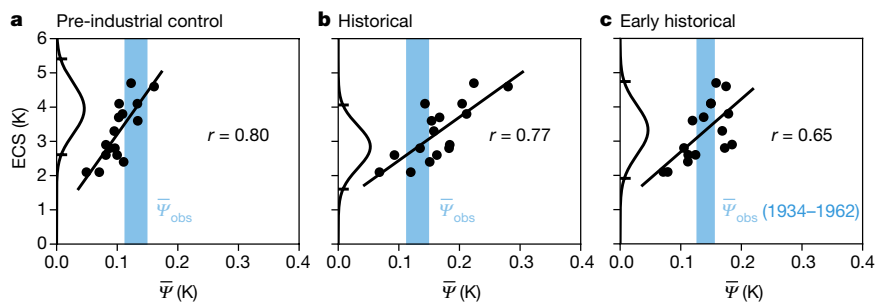


Fig. 1 | The ECS constraint depends on the underlying forcing.

a, Relationship between $\bar{\Psi}$ and ECS derived from the entire length of the pre-industrial control simulation available for each model. **b**, As in **a**, but for simulations of historical climate change over the period 1880–2016. **c**, As in **b**, but considering only global temperature data before 1963. In each panel, the black circles represent the original 16-model subset highlighted by Cox et al.¹. The black line is a linear fit and the vertical blue shading is the observational $\bar{\Psi}$ value (± 1 standard deviation). In

a and **b**, the observational range is derived from the entire temperature record (1880–2016), whereas the instrumental record before 1963 is used in **c** ($\bar{\Psi}$ values ending between 1934 and 1962). The implied probability distribution of ECS is displayed on the vertical axis. The median ECS value and 95% confidence interval for **a–c** are 4.0 ± 1.4 °C, 2.8 ± 1.2 °C and 3.3 ± 1.4 °C, respectively. The corresponding 95% confidence interval is denoted by horizontal lines along the y axis.

BRIEF COMMUNICATIONS ARISING

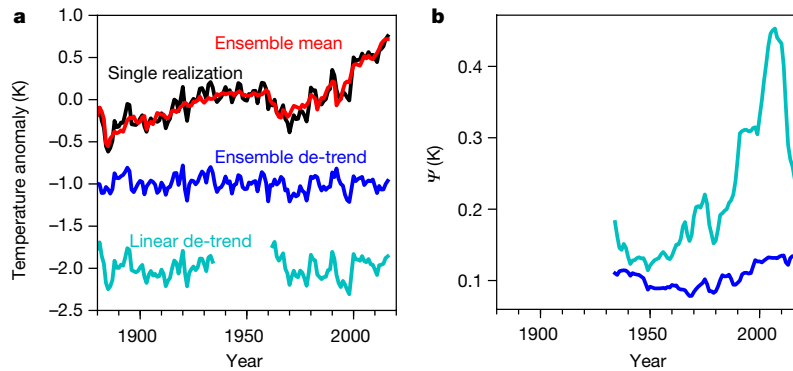


Fig. 2 | Forced temperature changes contaminate Ψ . **a**, Annual temperature anomaly of the CSIRO-Mk3-6-0 model for a single realization (black) and the ensemble average of ten realizations (red). The blue line shows the single realization de-trended using the ensemble average and the cyan line shows the first and last 55-year period of the single

realization de-trended using a linear fit. The blue and cyan lines are offset by -1 K and -2 K for clarity. **b**, Ψ values for the end of each 55-year period using a moving linear fit to remove forced temperature changes (cyan), and Ψ values calculated after first removing forced temperature variability (as represented by the ensemble average, blue).

the removal of the ensemble-mean forced signal (figure 2a in Cox et al.¹; Fig. 2b). The increase in Ψ occurs when there is a pronounced change in anthropogenic radiative forcing. Our results suggest that late twentieth-century forcing contaminates this variability-based constraint on ECS, undermining the physical interpretation of Ψ .

To understand the sensitivity of the ECS constraint to the time period selected, we consider the implications of using Ψ values from the early part of the historical record, before the rapid increase in anthropogenic forcing. We calculate $\bar{\Psi}$ from observational temperature data for the period 1880–1962, thus excluding forcing from the eruption of Mt Agung in 1963 (Fig. 1c). The resulting $\bar{\Psi}$ values are relatively small during the early historical period. The median ECS estimate is larger (3.3 °C; 95% confidence interval of 1.9 – 4.7 °C) than the result of Cox et al.¹ for the full historical record (2.8 °C). This indicates that the central ECS estimate and its bounds are sensitive to the time period considered.

The strength of the $\bar{\Psi}$ –ECS correlation is also sensitive to the subset of GCMs considered. If we include six additional models that were listed in extended data table 1 of Cox et al.¹ but were not included in the primary analysis, then the $\bar{\Psi}$ –ECS correlation decreases both in historical simulations ($r^2 = 0.59$ to $r^2 = 0.42$) and in pre-industrial control simulations ($r^2 = 0.63$ to $r^2 = 0.43$; Extended Data Fig. 1). Including additional GCMs that were not considered in the original research further degrades the $\bar{\Psi}$ –ECS relationship (Extended Data Fig. 1), indicating that the ECS variance explained by $\bar{\Psi}$ depends on the models considered. The justification for the smaller, 18-model subset was “to avoid biasing the emergent constraint towards the centres with the most model runs”. However, different models developed at the same centre can have widely varying $\bar{\Psi}$ and ECS values (Extended Data Fig. 1), so the inclusion of multiple models from the same institution does not necessarily weight $\bar{\Psi}$ and ECS values towards a particular centre. Our finding that the use of larger model subsets degrades the correlation between $\bar{\Psi}$ and ECS undermines the robustness of the constraint⁶.

Emergent constraints are most convincing when they are based on a solid theoretical understanding of the underlying physical mechanisms. The constraint presented by Cox et al.¹ was developed assuming that forced changes are negligible. As we have shown, their constraint is influenced by climate forcings in the latter half of the twentieth century. This introduces ambiguity in the interpretation of $\bar{\Psi}$. Despite this ambiguity, the fact remains that GCMs exhibit a relationship between $\bar{\Psi}$ and ECS. This suggests that $\bar{\Psi}$ may reflect an indirect constraint on ECS through a dependence on aerosol forcing⁸, volcanic response⁹ and

transient warming¹⁰. Although the original¹ Ψ constraint implies an ECS value near the centre of the likely range found by the Intergovernmental Panel on Climate Change (IPCC; 1.5 – 4.5 °C)¹¹, credible emergent-constraint studies¹² suggest ECS values that are greater than the likely estimate of Cox et al.¹. In the absence of additional efforts to understand the dependence of the constraint of Cox et al.¹ on climate forcing and model selection, $\bar{\Psi}$ alone does not provide a sufficient basis for narrowing the range of ECS reported by the IPCC, which is based on multiple lines of evidence¹¹.

Data availability

The datasets generated during this study are available from the corresponding author on reasonable request.

Code availability

The Python code used to produce the figures in this paper is available from the corresponding author on reasonable request.

Stephen Po-Chedley^{1*}, Cristian Proistosescu², Kyle C. Armour³ & Benjamin D. Santer¹

¹Lawrence Livermore National Laboratory, Livermore, CA, USA.

²Joint Institute for the Study of the Atmosphere and the Ocean, University of Washington, Seattle, WA, USA. ³Department of Atmospheric Sciences and School of Oceanography, University of Washington, Seattle, WA, USA.

*e-mail: pochedley1@llnl.gov

Received: 21 March 2018; Accepted: 11 July 2018

1. Cox, P. M., Huntingford, C. & Williamson, M. S. Emergent constraint on equilibrium climate sensitivity from global temperature variability. *Nature* **553**, 319–322 (2018).
2. Leith, C. E. Climate response and fluctuation dissipation. *J. Atmos. Sci.* **32**, 2022–2026 (1975).
3. Wigley, T. M. L. & Raper, S. C. B. Natural variability of the climate system and detection of the greenhouse effect. *Nature* **344**, 324–327 (1990).
4. Langen, P. L. & Alexeev, V. A. Estimating $2 \times \text{CO}_2$ warming in an aquaplanet GCM using the fluctuation-dissipation theorem. *Geophys. Res. Lett.* **32**, L23708 (2005).
5. Schwartz, S. E. Heat capacity, time constant, and sensitivity of Earth’s climate system. *J. Geophys. Res.* **112**, D24S05 (2007).
6. Klein, S. A. & Hall, A. Emergent constraints for cloud feedbacks. *Curr. Clim. Change Rep.* **1**, 276–287 (2015).
7. Kirk-Davidoff, D. B. On the diagnosis of climate sensitivity using observations of fluctuations. *Atmos. Chem. Phys.* **9**, 813–822 (2009).
8. Kiehl, J. T. Twentieth century climate model response and climate sensitivity. *Geophys. Res. Lett.* **34**, L22710 (2007).

BRIEF COMMUNICATIONS ARISING

9. Bender, F. A.-M., Ekman, A. M. L. & Rodhe, H. Response to the eruption of Mount Pinatubo in relation to climate sensitivity in the CMIP3 models. *Clim. Dyn.* **35**, 875–886 (2010).
10. Flato, G. et al. in *Climate Change 2013: The Physical Science Basis. Contribution of Working Group I to the Fifth Assessment Report of the Intergovernmental Panel on Climate Change* (eds Stocker, T. F. et al.) 741–866 (Cambridge Univ. Press, Cambridge, 2013).
11. Collins, M. et al. in *Climate Change 2013: The Physical Science Basis. Contribution of Working Group I to the Fifth Assessment Report of the Intergovernmental Panel on Climate Change* (eds Stocker, T. F. et al.) 1029–1136 (Cambridge Univ. Press, Cambridge, 2013).
12. Caldwell, P. M., Zelinka, M. D. & Klein, S. A. Evaluating emergent constraints on equilibrium climate sensitivity. *J. Clim.* **31**, 3921–3942 (2018).

Author contributions All authors collaborated on the design of the study, the interpretation of the results and writing the manuscript. S.P. performed the analysis using CMIP5 data.

Competing interests Declared none.

Additional information

Extended data accompanies this Comment.

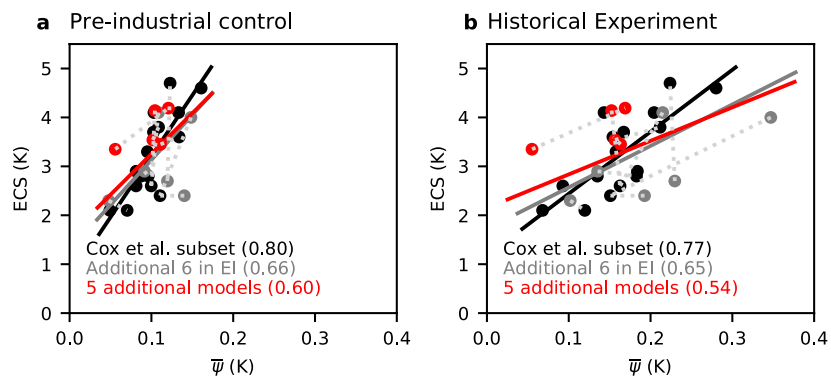
Supplementary information accompanies this Comment.

Reprints and permissions information is available at <http://www.nature.com/reprints>.

Correspondence and requests for materials should be addressed to S.P.

<https://doi.org/10.1038/s41586-018-0640-y>

BRIEF COMMUNICATIONS ARISING



Extended Data Fig. 1 | The strength of the $\bar{\Psi}$ -ECS relationship depends on the models considered. **a**, $\bar{\Psi}$ versus ECS for the pre-industrial control experiment (as in Fig. 1a), but including six additional models listed in extended data table 1 of Cox et al.¹ (grey) and five additional models not included in their original analysis (red; see Supplementary Information). The black line represents the regression obtained with the original 16-model subset of Cox et al.¹, the grey line represents the regression with

the 22-model subset (grey and black dots) and the red line represents the regression using all 27 models. The dotted grey lines connect models from a common modelling centre. The correlation coefficient is listed in parentheses for each set of models considered. **b**, As in **a**, but for the historical experiment. Using all models and the early historical period (1880–1962) to compute $\bar{\Psi}$ (as in Fig. 1c), we arrive at a median ECS of 3.4°C (95% confidence interval of 1.9–4.9°C).